

# Proteins with H-bond packing defects are highly interactive with lipid bilayers: Implications for amyloidogenesis

Ariel Fernández\*<sup>†‡§¶</sup> and R. Stephen Berry<sup>§||</sup>

\*Institute for Biophysical Dynamics, University of Chicago, Chicago, IL 60637; <sup>†</sup>Institute for Protein Research, Osaka University, 3-2 Yamadaoka, Suita, Osaka 565, Japan; and <sup>||</sup>James Franck Institute and Department of Chemistry, University of Chicago, Chicago, IL 60637

Edited by S. Walter Englander, University of Pennsylvania School of Medicine, Swarthmore, PA, and approved December 10, 2002 (received for review September 17, 2002)

**We noticed that disease-related amyloidogenic proteins and especially cellular prion proteins have the highest proportion of incompletely desolvated backbone H bonds among soluble proteins. Such bonds are vulnerable to water attack and thus represent structural weaknesses. We have measured the adsorption of proteins onto phospholipid bilayers and found a strong correlation between the extent of underwrapping of backbone H bonds in the native structure of a protein and its extent of deposition on the bilayer: the less the H bond wrapping, the higher the propensity for protein–bilayer binding. These observations support the proposition that soluble proteins with amyloidogenic propensity and membrane proteins share a pervasive building motif: the underwrapped H bonds. Whereas in membrane proteins, this motif does not signal a structural vulnerability, in soluble proteins, it is responsible for their reactivity.**

**B**ackbone amide–carbonyl H bonds (HB) become determinants of protein structure when the surrounding water is structured, immobilized, and ultimately removed (1–5). To estimate systematically the extent of desolvation of such bonds or their protection from water attack, we suggested counting the number of hydrophobic groups within a certain wrapping region of fixed volume around the HB (4). As shown in this work, native HB in soluble proteins are generally better wrapped than those of membrane proteins; they have to be to prevent water attack or simple destabilization by solvent exposure of the involved amide and carbonyl groups.

We also noticed exceptions to this general trait: disease-related amyloidogenic proteins (6–8) have a significantly lower average extent of HB protection than normal soluble proteins, with cellular prion proteins (9, 10) being the extreme examples of this anomaly. These results, reported here, may be relevant to help diagnose amyloidogenic propensity under physiological conditions, where some structural features are retained (11, 12). We suggest that the amyloidogenic propensity is reflected in the native structure, as implied by the correlation between amyloidogenic potential and structural instability (13, 14).

The significantly lower extent of HB wrapping in the native structure of amyloidogenic proteins and cellular prion proteins and the similar values we found for membrane proteins prompted us to investigate the extent of interaction between proteins and lipid bilayers by performing adsorption kinetic experiments under controlled hydrodynamic conditions (15). The extent of protein deposition on the lipid bilayer was found to be strongly correlated with the average extent of HB wrapping of the protein by hydrophobes, signaling a structural motif common to both unassociated amyloidogenic and membrane proteins: the underwrapped HB (UWHB).

This motif clearly signals what could be called a structural defect for soluble proteins. Thus, it is symptomatic that amyloidogenic proteins, which are unable to properly wrap their HB intramolecularly, would tend to aggregate in a supramolecular  $\beta$ -sheet structure dominated by stable unspecific intermolecular

wrapping of HB rather than specific side-chain interactions (7); UWHB appear to be essential factors determining protein instability and reactivity.

## Methods

**Determining the Average Extent of HB Desolvation from Data.** To determine the extent of HB wrapping or desolvation, we define desolvation spheres of radius  $R$  for a backbone HB by fixing  $R$  at 7.0 Å and centering the spheres at the  $\alpha$  carbons of the residues paired by the HB (4, 5). The inferences made are robust to moderate changes in the desolvation radius, holding within the range  $R = 7.0 \pm 0.3$  Å. An amide–carbonyl HB is defined by an N–O distance within the range 2.6–3.4 Å (typical extreme bond lengths) and a 45° latitude in the N–H–O angle.

To calculate the extent of wrapping of an HB, we count the number of hydrophobic residues (third bodies) whose side-chain center of mass lies within the wrapping spheres. The counting includes residues paired by the HB themselves if they happen to be hydrophobic. Thus, the HB wrapping is determined by three-body (hydrophobe–HB pair) correlations. Residues Ala, Leu, Ile, Val, Phe, Met, Trp, and Tyr are regarded as hydrophobic in accord with solvent-partitioning scales (16), and the center of mass for each residue is computed by averaging over all side-chain rotamers (17) using the native structures from the database described below.

The average extent of HB wrapping,  $\rho$ , is derived from two quantities:  $C_3$ , the total number of three-body correlations, and  $Q$ , the total number of backbone HB. Thus, we get  $\rho = C_3/Q$ . To obtain meaningful statistics, a sample of 2,808 structures from the Protein Data Bank was examined. Primary sequences were selected by using the OWL database, which emphasizes the removal of biasing redundancies (18). This method of estimating the HB wrapping gives an average  $\rho$  of 6.61 over the adopted database, with a dispersion  $\sigma = 1.46$  among backbone HB of a structure averaged over all sampled structures.

This computation of the extent of wrapping of a HB hinges on a somewhat arbitrary classification of residues; despite being polar, both K and, to a lesser extent, R have long aliphatic tails and thus might contribute to hydrophobic wrapping. Furthermore, the extent to which a residue contributes to the wrapping of a HB may depend on the number of its side-chain hydrophobic groups participating in the desolvation shell. This consideration suggests that the counting of the  $CH_n$  ( $n = 1, 2, 3$ ) groups in the desolvation domain might be a better measure of the extent of

This paper was submitted directly (Track II) to the PNAS office.

Abbreviations: HB, H bond; Hb, hemoglobin; UWHB, underwrapped HB.

<sup>‡</sup>On leave from Instituto de Matemática, Universidad Nacional del Sur-Consejo Nacional de Investigaciones Científicas y Técnicas de Argentina, Bahía Blanca 8000, Argentina.

<sup>§</sup>To whom correspondence may be addressed. E-mail: ariel@uchicago.edu or berry@uchicago.edu.

<sup>¶</sup>Present address: Department of Computer Science, Institute for Biophysical Dynamics, University of Chicago, 1100 East 58th Street, Chicago, IL 60637-1581.

wrapping. The average extent of wrapping in this case is  $\rho' = 19.62$  with a relatively narrower dispersion estimated at  $\sigma' = 3.05$ . Furthermore, the relative abundance of native folds according to their extent of wrapping has an inflection point at  $\rho' = 16.30$ , with 2,569 folds with  $\rho' > 16.30$ . When using the coarser measure, the inflection point is located at  $\rho = 6.20$  (see *Results*), and every fold for which  $\rho' > 16.30$  also satisfies  $\rho > 6.20$ . The converse is also true with three exceptions: angiogenin (PDB ID code 1b1e; PDB ID code 2ang  $\rho = 6.21$ ,  $\rho' = 16.10$ ), plasminogen (PDB ID code 1b2i,  $\rho = 6.22$ ,  $\rho' = 16.04$ ), and meizothrombin (PDB ID code 1a0h,  $\rho = 6.22$ ,  $\rho' = 16.02$ ). To the best of our knowledge, none of these proteins is amyloidogenic at least under physiological conditions.

In view of these similarities in the distribution of relative abundances, the coarser measure of wrapping as a marker aiding the diagnosis of amyloidogenic propensity (see *Results*) seems quite adequate. This must be attributed in part to the specific chemical compositions of natural protein chains and also to the fact that the polar groups at the ends of both K and R would have very high self energy unless they are extensively solvated by bulk-like water. This free-energy minimization by hydration in turn leads to a straightening of the K and R side chains, lowering the local protection that these side chains can actually bring to the backbone. Furthermore, 69% of the UWHB detected involve at least one of the following four polar residues: D, S, T, or N. The polar groups of these residues are attached directly to the  $\beta$  carbon and thus do not allow for any protective clustering of hydrophobic groups around the backbone, as such arrangements would dramatically increase the self-energy of the polar groups and hinder or even prevent their solvation. This justifies our exclusion of polar groups as HB protectors in our measures of wrapping.

**Protein Adsorption Experiments.** Protein adsorption at a solid-liquid interface under controlled hydrodynamic conditions was monitored by using an optical biosensing device based on evanescent field total reflection (11, 19, 20). The experiment was designed to measure the affinity of specific proteins for lipid bilayers. A Langmuir-Blodgett lipid bilayer (21) was deposited onto a TiO<sub>2</sub>/SiO<sub>2</sub>-coated waveguide of a wide diffraction grating (period 412 nm, Harrick Scientific, Ossining, NY). The flow cell (flow rate, 1.36 mm<sup>3</sup>/s; constant bulk concentration,  $6 \times 10^{14}$  protein molecules per cm<sup>3</sup>) of semicircular cross-section was mounted on a bilayer-coated waveguide, which thus became a wall of the cell. The time dependence of protein uptake was monitored by optical interrogation of the protein adlayer without interference from bulk fluctuations or convective perturbations of the diffraction pattern. The optical detection is based on the fact that the evanescent field interacts only with a region extending just a fraction of the wavelength away from the waveguide surface. The waveguiding TiO<sub>2</sub>/SiO<sub>2</sub> coat was 180 nm thick, and the polarized light beam was produced by an He/Ne laser ( $\lambda = 632.8$  nm, Spectra-Physics). Thus, only discrete modes exist in the total reflection spectrum, which was recorded by using a Shimadzu instrument (model PC1200).

The number of adsorbed protein molecules per  $\mu\text{m}^2$  was determined from the thickness and refractive index of the protein adlayer, as specified in ref. 15. The six proteins examined,  $\beta$ -lactoglobulin, apomyoglobin, egg-white lysozyme,  $\beta_2$ -microglobulin, human insulin, and apolipoprotein A-I, were 99% pure (Sigma). All measurements were made at  $T = 293$  K by using a single buffer (0.01 M Hepes/0.7 mM EDTA, pH 7.1; refractive index = 1.33301 for  $\lambda = 632.8$  nm). The choice of phospholipid bilayer was made to minimize the distortion of the bilayer orientation (22) and even bilayer destruction, which might result on deposition of proteins with high densities of structural defects (insulin, apolipoprotein). Another consideration for the choice of lipid bilayer is its mechanical stability

under the hydrodynamic conditions adopted. Short ( $n < 10$ ) fatty acid chains are less prone to distortion on protein deposition but are mechanically more unstable. Thus, we found that a good compromise between the conflictive effects was achieved with 1,2-dilauroyl-sn-glycero-3 phosphatidylcholine (Avanti Polar Lipids).

## Results and Discussion

**HB Packing Deficiencies and Amyloidogenic Proteins.** Because HB seem to be stable only when surrounded by an environment where water is excluded or highly structured, it is informative to determine their average extent of desolvation over many protein structures. This parameter can then be averaged over a statistical ensemble of protein structures to determine the typical environment of a HB. This average environment, in turn, enables us to define and identify UWHB, which are highly relevant to our present study.

A HB environment is operationally defined (with our coarser method) by the number of hydrophobic residues (third bodies) contained within the 7-Å-radius spheres centered at the  $\alpha$  carbons of the residues paired by the HB (see *Methods*). Thus, the number of three-body hydrophobe-HB residue pair correlations characterizes an HB environment: a hydrophobic side chain whose center of mass is contained within the desolvation sphere of a HB is counted as a correlation.

As stated previously, the average extent,  $\rho$ , of HB wrapping for a single protein, as defined above (see *Methods*), over the 2,808-structure sample, is 6.61, and its dispersion among backbone HB of a structure averaged over all sampled structures is  $\sigma = 1.46$ . The more elaborate measure  $\rho'$  gave statistics essentially consistent with these.

These statistics dictate a way to define UWHB as those at the lower extreme of the distribution, containing two or fewer hydrophobes in their wrapping spheres. Alternative ways to compute the extent of desolvation of HB yield a narrower spread of  $\rho$  values (4), but the one chosen for this study seems satisfactory to optimize the distinction between normal and amyloidogenic proteins. The previous estimate put the average value of  $\rho$  closer to 5.

Fig. 1 displays the UWHB for hemoglobin (Hb)  $\beta$ -subunit (PDB ID code 1bz0, chain B). Within the natural interactive context of the Hb subunit, the UWHB signal crucial binding regions (23); UWHB (Glu-90, Asp-94), (Glu-90, Lys-95) are associated with the  $\beta$ -FG corner involved in the quaternary  $\alpha_1\beta_2$  interface. UWHB (Pro-5, Ser-9) is adjacent to Glu-6, which, in sickle cell anemia, mutates to Val-6 and is located at the Val-6-(Phe-85, Leu-88) interface in the deoxyHbS fiber.

Fig. 1 suggests that most UWHB occur at solvent-exposed elbows or sharp turns, well known to be good candidates for intermolecular interaction (23). However, that is not always the case. For example, in cellular prion proteins, which are the worst wrappers of HB among soluble proteins (Fig. 2), the UWHB occur extensively along entire helices, whereas in neurotoxins, entire  $\beta$ -sheets are underwrapped. The wrapping of the HB may be viewed as an element of cooperativity (5); the occurrence of a prevailing HB in a stable structure is not simply the result of a local folding event bringing two residues to proximity. Rather, such a bond requires a protective desolvation shell, which involves a larger-scale organization of the chain. Thus, the UWHB represent regions where a basic building constraint is not fulfilled.

The distribution of proteins according to their average extent of HB wrapping is shown in Fig. 2. The sample of 2,808 proteins is large enough to define a reliable probability distribution with an inflection point at  $\rho = 6.20$ . The integration of the probability distribution over a  $\rho$ -interval gives the fraction of proteins whose  $\rho$  lies within that range. Of the 2,808 proteins examined, 2,572 have  $\rho > 6.20$ , and none of these is known to yield amyloid

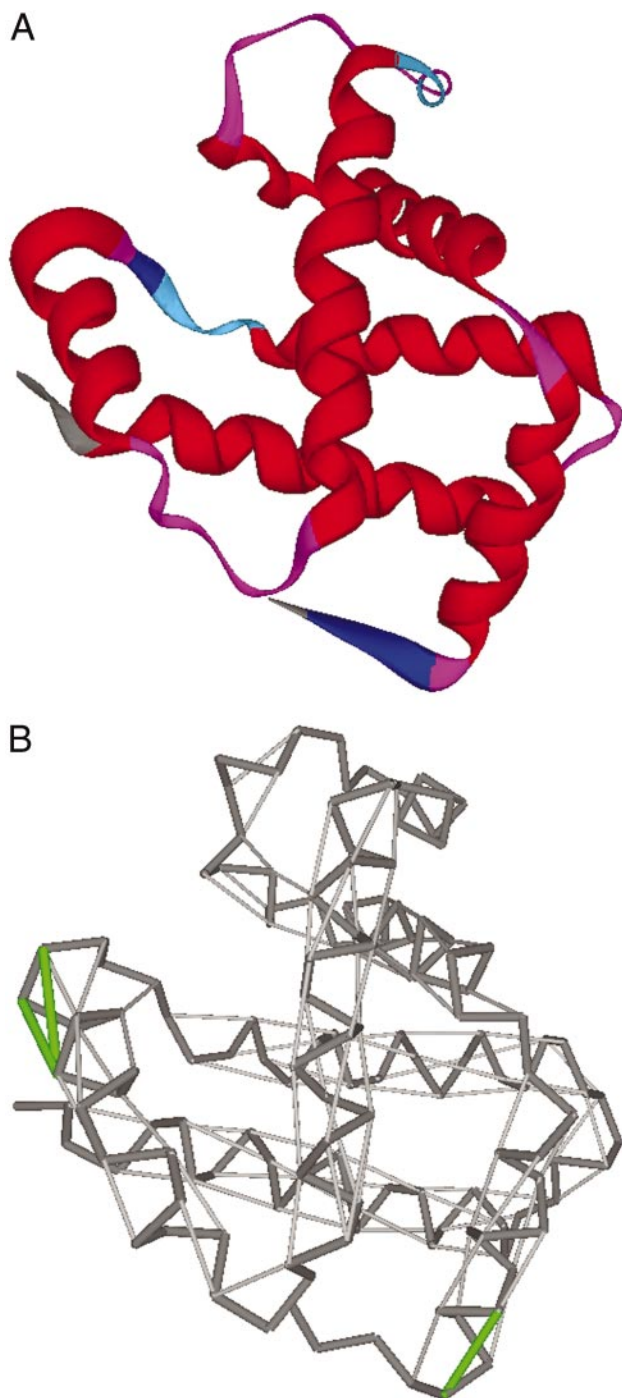


**Fig. 1.** (A) Ribbon display of Hb  $\beta$  subunit in its native conformation. (B) Pattern of sufficiently wrapped HB (light gray segments joining  $\alpha$  carbons of residues paired by the HB) and UWHB (green segments) for Hb  $\beta$  subunit. The virtual backbone bonds between  $\alpha$  carbons define the dark gray polygonal.

aggregation under physiological conditions providing at least partial retention of structure. Strikingly, the known disease-related amyloidogenic proteins are found in the comparatively underpopulated  $3.5 < \rho < 6.20$  range, with the cellular prion proteins located at the extreme of the spectrum ( $3.53 < \rho < 3.72$ ). This analysis reveals that an overall partial exposure of HB to water attack might be a necessary condition to induce organized aggregation and that, at most, 10% of Protein Data Bank proteins may possess this propensity. This fact has proven

useful in the diagnosis of disease-related amyloidogenic propensity (A.F., J. Kardos, and Y. Goto, unpublished results).

The range of HB wrapping  $3.5 < \rho < 4.6$  associated with 17 sampled Protein Data Bank membrane proteins reveals that such proteins do not have the stringent HB packing requirements of soluble proteins. Thus, as hinted by the experimental results reported here, it is expected that at least some soluble proteins with an overall severe underwrapping of their HB (likely in the range  $3.5 < \rho < 4.6$ ) might exhibit some tendency to form ion channels *in vitro* (24). The virtually identical  $\rho$  value for human prion and outer membrane protein-A (PDB ID code 1bxw,  $\rho = 3.7$ ) is revealing in this regard.

Furthermore, all known amyloidogenic proteins that occur naturally in complexed form have sufficient HB wrapping when they form their respective complexes ( $\rho$  values near 6.2). Their amyloidogenic propensities only manifest themselves under conditions in which the protein is dissociated from the complex (see Fig. 2). This fact is corroborated by performing the following computation. Suppose an intramolecular HB is underwrapped within the isolated protein molecule but located at an interface on complexing. To determine its extent of wrapping within the complex, we add to the count the additional third-body hydrophobic residues of the binding partner that lie within the desolvation spheres of the intramolecular HB. Thus, the uncomplexed  $\beta_2$ -microglobulin (PDB ID code 1i4f) (25, 26) has  $\rho = 5.2$ , which places it high in the purported amyloidogenic region. However, on complexing within the MHC-I, its  $\rho$  value increases to 6.22.

**HB Packing Deficiency and Protein–Membrane Interaction.** As a result of the site-specificity of complexing, certain UWHB in the isolated protein may complete their desolvation shells and gain stabilization, as indicated above. However, for a given protein, the structure of its complexed state informs us only on its interaction with a single binding partner; nothing can be inferred about the role of structurally defective HB not contained in a specific binding site. To understand the role of UWHB, we would need to know the entire interactive context of the protein, i.e., all its purported ligands and even the crystal contacts made by the different complexes, and check whether the desolvation shells of the defective HB are filled or completed on the different interactions, a daunting task.

One way of circumventing this problem is presented in this work. To obtain an average picture of the interactive context of a protein defined by its structural defects, we measured the extent of adsorption of the protein on a phospholipid bilayer and correlated the result with the average extent of underwrapping of the native HB in the uncomplexed protein. Regardless of the adsorption mode, it is clear that exposed (UW) HB, which are necessarily on the protein surface, should anchor a successful landing, because their vulnerability to water attack decreases with the attachment of the protein to the bilayer surface.

No information can be clearly extracted from our measurements on the exact mode of adsorption or the extent of denaturation of the protein on binding to the bilayer. However, the significant linear correlation found between adsorption uptake at long equilibration times and average extent of HB wrapping (Figs. 3 and 4) suggests the following picture. A successful or sticky landing of the protein molecule on the bilayer is directly correlated with the probability that the contact region contains UWHB. Thus, the higher the proportion of UWHB (the lower the  $\rho$  value), the higher the extent of adsorption. This picture provides a solid *a posteriori* justification for our approach: It is clear that proteins which are highly defective in terms of underprotected HB are also prone to be adsorbed as a means to compensate for the imperfect HB packing in the native fold. This result holds regardless of whether or not the native structure is

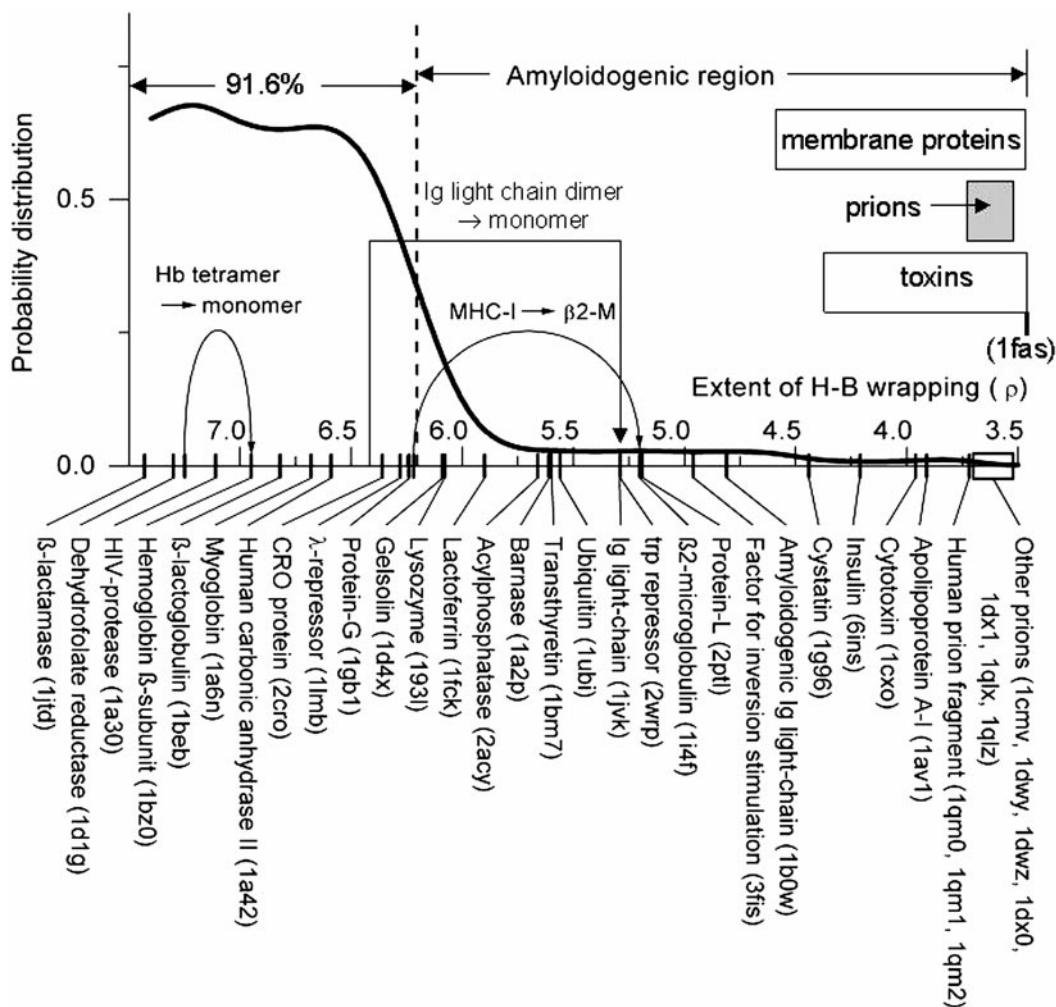


**Fig. 2.** Distribution of soluble proteins according to their average extent of HB wrapping  $\rho$ . The probability density distribution was obtained from a large nonredundant Protein Data Bank sample (see *Methods*). Its integration over a  $\rho$ -interval or range gives the fraction of proteins whose  $\rho$  value lies in the interval. The number of isolated soluble proteins with extent of wrapping lower than the inflection point marked by a dashed line ( $\rho < 6.20$ ) is  $\approx 10\%$  of the sample. Representative proteins identified by their respective Protein Data Bank ID codes are displayed in the abscissas. The change in  $\rho$  on dissociation of a complex is indicated by a curved arrow in two illustrative cases: the  $\beta$ -subunit of Hb taken from complexed to isolated form and the  $\beta_2$ -microglobulin within the MHC-I complex and taken in isolation.

ultimately retained or lost as the protein becomes progressively integrated with the bilayer.

Six commercially available proteins spread over the entire  $\rho$  spectrum in their uncomplexed form were chosen for the study. Two of them,  $\beta$ -lactoglobulin ( $\rho = 6.72$ ) and apomyoglobin ( $\rho = 6.65$ ), are not known to be amyloidogenic under physiological conditions, whereas the others, lysozyme ( $\rho = 6.10$ ),  $\beta_2$ -microglobulin ( $\rho = 5.21$ ), human insulin ( $\rho = 4.21$ ), and apolipoprotein A-I ( $\rho = 3.9$ ), definitely are (6–8). The adsorption kinetics for each of the six proteins, monitored by the number of adsorbed molecules per  $\mu\text{m}^2$ , are shown in Fig. 3. Adsorption was relatively slow but nearly irreversible in five cases, reaching a plateau at approximately  $t = 10^3$  s. The lowest affinity was observed for the protein with the highest  $\rho$  value:  $\beta$ -lactoglobulin.

A clear trend is apparent from Fig. 3: the lower the average extent of HB protection, the higher the extent of adsorption. The densities of adsorbed molecules were normalized to account for the different protein sizes, as indicated in the figure legend. Thus,  $\rho$  can be straightforwardly related to the plateau density of adsorbed molecules at  $t = 10^3$  s, which ranges from  $3 \times 10^3$  molecules per  $\mu\text{m}^2$  for apomyoglobin or irreversibly adsorbed

$\beta$ -lactoglobulin, to  $3.7 \times 10^4$  for apolipoprotein A-I. In fact, both parameters are strongly correlated and best fitted by a linear dependence, as shown in Fig. 4.

A similar linear fit, only with a 12% narrower confidence band, may be obtained by correlating the adsorption uptake at 1,000 s with the finer-grain measure of the extent of wrapping ( $\beta$ -lactoglobulin,  $\rho' = 20.7$ ; apomyoglobin,  $\rho' = 19.8$ ; egg-white lysozyme,  $\rho' = 18.1$ ;  $\beta_2$ -microglobulin,  $\rho' = 15.5$ ; insulin,  $\rho' = 12.9$ ; apolipoprotein,  $\rho' = 12.1$ ), described in *Methods* (see ref. 27).

Taken together, the results presented in Figs. 2–4 signal a relationship between disease-related amyloidogenic propensity, extent of defective packing of native HB, and affinity for protein–membrane interactions. The experiments were motivated by the basic observation that backbone HB in amyloidogenic proteins are on average more deprived of proper protection from water attack than those of normal soluble proteins. This trait was found to be extreme in prion proteins.

The correlation shown in Fig. 4 provides an average picture of the role of structural defects in determining the extent of protein–membrane interactions and singles out a structural motif common to membrane and amyloidogenic proteins: the backbone UWHB.

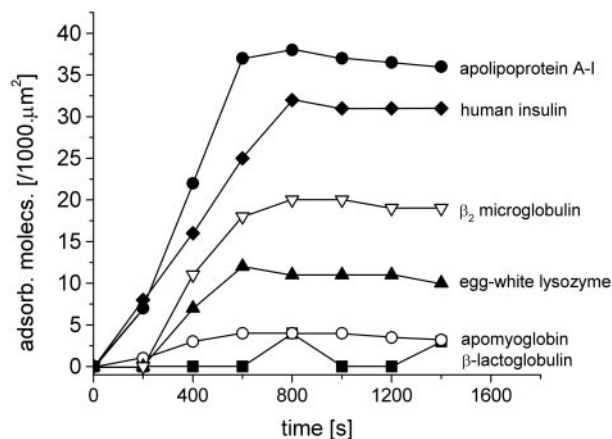


**Fig. 3.** Kinetics of protein adsorption onto a 1,2-dilauroyl-sn-glycero-3-phosphatidylcholine lipid bilayer (see *Methods*) determined by monitoring the density of adsorbed protein molecules (given in thousands of molecules per  $\mu\text{m}^2$ ). Six cases were studied: apolipoprotein A-I, human insulin,  $\beta_2$ -microglobulin, egg-white lysozyme, apomyoglobin, and  $\beta$ -lactoglobulin. The densities of adsorbed molecules given in the ordinates were normalized by multiplying the measured values by the scaling coefficient:  $c = [\text{solvent-exposed area of protein molecule}]/[\text{solvent-exposed area of } \beta\text{-lactoglobulin molecule}]$  (i.e., adopting  $\beta$ -lactoglobulin as the standard protein). ●, apolipoprotein A-I; ◆, human insulin; ▽,  $\beta_2$ -microglobulin; ▲, egg-white lysozyme; ○, apomyoglobin; ■,  $\beta$ -lactoglobulin.

Whereas in the former, such motif does not signal a structural vulnerability, in the latter it does, as exposed HB are prone to water attack. Thus, the UWHB becomes a determinant of protein reactivity, which could manifest alternatively as pathogenic aggregation or interaction with the membrane.

**Implications for *in Vivo* Protein Folding.** Finally, we speculate on how our results may carry implications regarding *in vivo* folding pathways. It seems that unprotected HB are sticky, that is, they tend to induce localized association to a lipid bilayer site as a possible means to desolvate and thus protect against solvent attack. Consequently, a compliant lipid-layered structure, such as that in the cytosol, may dynamically wrap and protect HB in transient intermediate folds until the protein chain is organized enough to be able to protect them intramolecularly. To avoid hindering the folding process, the dynamic intermolecular protection must be transient, a property that requires flexibility of the cytoplasmic membranes. Furthermore, we suspect this could involve a hierarchical process, first local folding, then global, under *in vivo* conditions. This is so simply because partially protected local structures may persist, when dynamically assisted by the cytoplasmic lipid bilayers, until the full protection of tertiary structure forms. This scenario should be testable experimentally by designing an environment resembling *in vivo* conditions, dense with flexible liposome vesicles, and probing with circular dichroism and fluorescence to monitor the conformational changes in the protein chain, especially those induced by transient association with the membranes.

A hierarchic scenario *in vivo* seems even more likely than one *in*

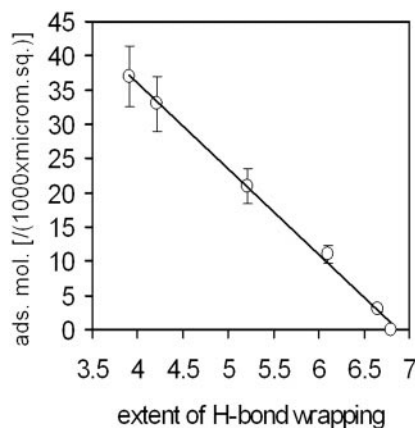


**Fig. 4.** Normalized number of adsorbed molecules per  $\mu\text{m}^2$  at  $t = 10^3$  s for six different proteins correlated with  $\rho$ , the average extent of HB desolvation of the respective native protein structures. The circles with error bars correspond to apolipoprotein A-I ( $\rho = 3.9$ ), human insulin ( $\rho = 4.21$ ),  $\beta_2$ -microglobulin ( $\rho = 5.21$ ), egg-white lysozyme ( $\rho = 6.1$ ), apomyoglobin ( $\rho = 6.6$ ), and  $\beta$ -lactoglobulin ( $\rho = 6.72$ ). The adsorption process reached a stationary state by  $t = 10^3$  s and remains essentially irreversible, as revealed by Fig. 3, with the exception of  $\beta$ -lactoglobulin, which shows low affinity for the surface and cycles of adsorption and nearly complete desorption. The error bars signal uncertainty in the measurements stemming from the signal/noise ratio in the spectrometric measurements, which translates into a resolution of  $5 \times 10^8$  adsorbed molecules per  $\text{mm}^2$ .

*vitro*, where the solvent plays no role in helping to protect packing defects around formed HB (28, 29). Thus, it seems that protein folding under *in vitro* conditions may require almost simultaneous desolvation of most of the HB, a process that would require a large-scale organization. The protein molecule *in vitro* would have to go through a lot of trial and error to find that organization needed to generate an overall protective topology. We suspect this is the reason for the two-stateness observed in the *in vitro* folding of moderate-size proteins (30). We predict that this two-stateness should not hold under *in vivo* or quasi *in vivo* conditions, where no significant kinetic-entropic barrier should be present.

One other aspect of *in vivo* phenomena to which these results may be relevant concerns the possibility that protein-membrane complexes, bound by HB protections, could play a significant role in nucleation of amyloid fibrils. That membranes could bind individual strands and thereby bring them into proximity despite their low concentration in solution had been suggested (D. J. Gordon, J. J. Balbach, R. Tycko, and S. C. Meredith, personal communication); the mechanism described here would provide a molecular basis for such binding. Our analysis implies that an agent to suspect as the pathogen may be the protofibril rather than the fibril. The protofibril, with its UWHB, can penetrate the membrane, whereas the well wrapped fibril cannot.

A.F. thanks Professor Yuji Goto for hospitality during his tenure of a Visiting Professorship at Osaka University and Profs. Jeremy Ramsden (Cranfield University, Cranfield, U.K.) and Axel Blau (University of Kaiserslautern, Kaiserslautern, Germany) for technical assistance and enlightening discussions. R.S.B. acknowledges the support of the National Science Foundation.

- Nemethy, G., Steinberg, I. Z. & Scheraga, H. A. (1963) *Biopolymers* **1**, 43–69.
- Vila, J. A., Ripoll, D. R. & Scheraga, H. A. (2000) *Proc. Natl. Acad. Sci. USA* **97**, 13075–13079.
- Fernández, A., Colubri, A. & Berry, R. S. (2002) *Phys. A* **307**, 235–259.
- Fernández, A. & Berry, R. S. (2002) *Biophys. J.* **83**, 2475–2481.
- Fernández, A., Sosnick, T. R. & Colubri, A. (2002) *J. Mol. Biol.* **321**, 659–675.
- Rochet, J. C. & Lansbury, P. T., Jr. (2000) *Curr. Opin. Struct. Biol.* **10**, 60–68.
- Dobson, C. M. (1999) *Trends Biochem. Sci.* **24**, 329–332.

- Koo, E. H., Lansbury, P. T., Jr., & Kelly, J. W. (1999) *Proc. Natl. Acad. Sci. USA* **96**, 9989–9990.
- Prusiner, S. B. (1998) *Proc. Natl. Acad. Sci. USA* **95**, 13363–13383.
- Zahn, R., Liu, A., Luhrs, T., Riek, R., von Schroetter, C., Lopez-Garcia, F., Billeter, M., Calzolari, L., Wider, G. & Wuthrich, K. (2000) *Proc. Natl. Acad. Sci. USA* **97**, 145–150.
- Verdone, G., Corazza, A., Viglino, P., Pettirossi, F., Giorgetti, S., Mangione, P., Andreola, A., Stoppini, M., Bellotti, V. & Esposito, G. (2002) *Protein Sci.* **11**, 487–499.

12. Chamberlain, A. K., Receveur, V., Spencer, A., Redfield, C. & Dobson, C. M. (2001) *Protein Sci.* **10**, 2525–2530.
13. Booth, D. R., Sunde, M., Bellotti, V., Robinson, C. V., Hutchinson, W. L., Fraser, P. E., Hawkins, P. N., Dobson, C. M., Radford, S. E., Blake, C. C. & Pepys, M. B. (1997) *Nature* **385**, 787–793.
14. Souillac, P. O., Uversky, V. N., Millett, I. S., Khurana, R., Doniach, S. & Fink, A. L. (2002) *J. Biol. Chem.* **277**, 12657–12665.
15. Ramsden, J. J. (1993) *J. Stat. Phys.* **73**, 853–877.
16. Fauchere, J. & Pliska, V. (1983) *Eur. J. Med. Chem.* **18**, 369–375.
17. Fernández, A. & Colubri, A. (2002) *Proteins* **48**, 293–310.
18. Bleasby, A. J., Akrigg, D. & Attwood, T. K. (1994) *Nucleic Acids Res.* **22**, 3574–3577.
19. Ramsden, J. J., Bachmanova, G. I. & Archakov, A. I. (1996) *Biosens. Bioelectron* **11**, 523–528.
20. Suci, P. A. & Geesey, G. G. (2001) *Langmuir* **17**, 2538–2540.
21. Roberts, G. G., ed. (1990) *Langmuir–Blodgett Films* (Plenum, New York).
22. Yamaguchi, S., Hong, T., Waring, A., Lehrer, R. I. & Hong, M. (2002) *Biochemistry* **41**, 9852–9862.
23. Voet, D. & Voet, J. G. (1990) *Biochemistry* (Wiley, New York).
24. Hirakura, Y. & Kagan, B. (2001) *Amyloid* **8**, 94–100.
25. Hoshino, M., Katou, H., Hagihara, Y., Hasegawa, K., Naiki, H. & Goto, Y. (2002) *Nat. Struct. Biol.* **9**, 332–336.
26. McParland, V. J., Kalverda, A. P., Homans, S. W. & Radford, S. E. (2002) *Nat. Struct. Biol.* **9**, 326–331.
27. Rose, G. D. & Roy, S. (1980) *Proc. Natl. Acad. Sci. USA* **77**, 4643–4647.
28. Fernández, A. (2002) *J. Biomol. Struct. Dyn.* **19**, 735–737.
29. Baldwin, R. L. & Rose, G. (1999) *Trends Biochem. Sci.* **24**, 26–33.
30. Krantz, B. & Sosnick, T. R. (2000) *Biochemistry* **39**, 11696–11701.